Costas Loop Demodulation of Suppressed Carrier BPSK Signals in the DSN Environment—Experimental Results Obtained at TDL

R. Reasoner
DSN Data Systems Section

G. Stevens and K. T. Woo
Communications Systems Research Section

Suppressed carrier binary phase-shift keyed (BPSK) signalling is currently being considered as a design alternative for future DSN telemetry in the multimegabit range. Carrier tracking of such signals is usually achieved by a Costas loop, as opposed to the ordinary phase lock loop. A Costas loop capable of demodulating BPSK signals with data rates up to 1 Msps has been designed and constructed and its Doppler tracking performance with respect to a Block III receiver has been tested at the Telecommunications Development Laboratory (TDL). The purpose of these experiments is to investigate the compatibility of suppressed carrier signalling with the current radio metric system; specifically Doppler tracking and ranging. This article documents the experimental results obtained to-date with respect to Doppler tracking.

I. Introduction

In future imagery missions such as VOIR, the symbol rates of the returned telemetry data are expected to be in the multimegabit per second region. In this range of data rates, it is pointed out in Ref. 1 that, from the telemetry systems point of view, suppressed carrier binary phase-shift keyed (BPSK) signalling with Costas loop carrier recovery will offer advantages both in bandwidth savings and improved tracking performance over the residual carrier format. However, the compatibility of this approach with the existing radio metric system has not been verified. The basic concerns here are the Doppler tracking and ranging accuracies, and their sensitivities to data rates, data patterns, temperature variations, and Doppler conditions. Also, when the Costas loop is used in conjunction with one of the DSN receivers, the effects of hardware constraints peculiar to these receivers such as passband characteristics, mixer nonlinearities, and oscillator phase instabilities on this new type of signal format are also of concern in the overall system performance.

To investigate these effects on system performance it is felt that, aside from detailed analyses, which are only as accurate as the models assumed, actual testing of a Costas loop performing carrier recovery for suppressed carrier signals in the DSN environment is most beneficial.

A scaled-down version of the Costas loop that will be implemented in the multimegabit telemetry demodulator/detector (MTDD) has been designed and constructed. The symbol rates of the MTDD range from 100 kilosymbols per second (ksps) to 30 megasymbols per second (Msps) (Ref. 2). The Costas loop described here is capable of demodulating BPSK signals with data rates up to 1 Msps only. A detail description of this Costas loop is documented in Ref. 3. This loop has been tested with respect to the Block III receiver at TDL. So far, the tests performed concern only Doppler tracking. Four categories of tests have been performed. The first category consists of design verifications of the Costas demodulator. This consisted of measuring the loop's rms phase jitter and steady-state phase error at assumed Doppler conditions and various symbol SNRs (ST/N_0). Their sensitivities with respect to data pattern and data rate variations were investigated as were the loop's frequency pull-in time and pull-in range. The pull-in time and range tests serve only to verify the design, since sweep acquisition is planned in the MTDD unit.

The second category of tests consists of long-term stability tests of the Costas loop in the TDL environment, which closely approximates that of the DSN stations. The third category of tests was designed to test the variations in the phase of the Costas loop's reconstructed carrier due to Doppler offsets and the effects of asymmetric passband filtering in the receiver front end (e.g., the maser amplifier). The fourth category of tests was designed to investigate the performance of the Costas loop when used for carrier recovery of residual carrier signals with an 80-deg modulation angle and with data on a square-wave subcarrier. The Voyager spacecraft transmits signals of this type.

The test results obtained at the TDL with respect to these tests are documented in this paper. These preliminary results indicate that there is no noticeable incompatibility between the current radio metric system and Costas loop demodulation of suppressed carrier BPSK signalling, as far as Doppler tracking is concerned. Of course, further testing has to be performed with respect to ranging accuracies.

II. Description of Test Configurations

The Telecommunications Development Laboratory (TDL) was employed to test the performance of this Costas demodulator. The TDL contains the equipment necessary to generate BPSK signals at S- and X-band, Block III and Block IV receivers, Doppler extractors, and the capability to perform automated phase data gathering and analysis. The Block III receiver was selected over the Block IV receiver for our measurements due to hardware problems in the Block IV during the test period.

Figure 1 indicates the configuration used to generate BPSK S-band signals. The Data Rate Synthesizer and Subcarrier Generator are locked to the Frequency and Timing Subsystem (FTS) that provides reference tones for the TDL. The Data Rate Synthesizer and Subcarrier Generator are manually programmed to the desired data rate and subcarrier frequency, respectively. The Data Pattern Generator is manually set to either a PN sequence or a switch selected data pattern. Either the modulated subcarrier or the data pattern itself may be selected to modulate the carrier.

The Block III Exciter is also shown in Fig. 1. The exciter output is monitored by a frequency counter to provide equivalent Doppler information (frequency counted × 96 = carrier frequency at S band). The signal level to the modulator is varied to adjust for the desired carrier suppression. The output from the translator circuit is the S-band downlink signal.

Figure 2 depicts the receiver end of the configuration. The S-band signal is attenuated to a desired level based on Y factor measurements at the 50 MHz IF output. The output from the 10-MHz IF is fed to a narrowband measurement system to measure the carrier suppression by testing the power at the carrier frequency with and without modulation. The 10-MHz IF output drives the Block III receiver control loop and the Costas control loop. The Block III receiver VCO is driven by either loop by connecting the appropriate cables.

Detail descriptions of the Costas loop design can be found in Ref. 3. For the particular loop that was intended only for testing purposes at TDL, no automatic gain control circuit was provided. The manual gain control (MGC) in the Block III was therefore used in testing this Costas loop.

Figure 3 shows the data acquisition hardware. The Doppler extractor is fed by the exciter and receiver oscillator outputs (each tripled). The extractor simulates the up and down conversions as well as the spacecraft transponder. The signals are mixed to 50 MHz (in lock), divided by 4, and complex mixed against 12.5 MHz to provide a phase error/4 signal and a phase error/4 + 90 deg signal. These signals are fed to two analog-to-digital converters (A/D) that are controlled by an Altair 8800 microcomputer. The 8800 is initialized by, and transmits digital information to, a Modcomp II minicomputer.

The software available at TDL has the capability to provide mean phase (for long-term stability) and phase jitter (for rms) analyses.

III. Performance Verification Tests

The first set of tests performed was intended to verify the predicted performance of the Costas loop design.

Before installing the Costas loop in the TDL, the hardware was tested with simulated, noise-free signals. A 10-MHz biphase modulated suppressed carrier signal was generated with the equipment shown in Fig. 4. The frequency and phase of the 10-MHz carrier oscillator was controlled by the Costas loop hardware. In particular, pull-in time of the Costas loop was measured by stepping the carrier frequency oscillator in known increments. Results of these tests are shown in Table 1. Also shown in Table 1 are the theoretical predictions on these pull-in times, which are derived in Ref. 3. The particular loop design with a received data rate of 100 ksps (Ref. 3) was used in obtaining the test data shown here.

As shown in Table 1, reasonable agreement in the pull-in time performance between predictions and measurements were obtained. Also measured was the pull-in range of the loop. The measured pull-in range was around 1000 Hz. The predicted pull-in range is 894 Hz (Ref. 3).

After the Costas loop was installed at TDL, interfacing with the 10-MHz IF of the Block III receiver, its performance was tested in the presence of thermal noise and oscillator phase instabilities. To verify its performance, the rms phase jitter and steady-state phase errors of the loop were first tested as functions of the following variables:

(1) Data patterns (PN or square wave)

(2) Data rates (100 ksps to 1 Msps)

(3) Symbol SNRs (from −4 dB to +4 dB)

The rms phase jitter of the Costas loop was tested with the configurations shown in Figs. 1, 2, and 3. Figure 5 shows the rms phase jitter of the loop as ST/N_0 increases from −4 to +4 dB. The loop was designed for the 100 ksps data rate. Test results for both PN and square wave data are shown. The results shown in Fig. 5 demonstrated good agreement between predicted and measured performance. They also demonstrated that the loop's performance is practically insensitive to whether the data pattern is PN or square wave. Agreement between predictions and measurements are better at high ST/N_0s than at low ST/N_0s. This can be attributed to the effects of oscillator phase instabilities, since, at low ST/N_0s signal suppression due to the hard-limiter in the in-phase channel (Ref. 3) of the Costas loop is more severe, resulting in narrower loop bandwidths and larger phase jitter due to oscillator phase instabilities. The performance predictions given in Ref. 3 treated the effects of thermal noise only, while the oscillator phase noise effects were neglected.

Figure 6 shows the rms phase jitter of the three loops designed for data rates at 100 ksps, 250 ksps, and 1 Msps respectively, as functions of ST/N_0. By design, the theoretical performance of these loops should be identical. However, measured results show that the phase jitters of the loops at higher data rates are larger than those of the lower data rate cases. This is due largely to the inherent bandlimiting of the complex mixer (Ref. 3). In addition, this may also be due, though much less significantly, to the data generator that generates less perfect waveforms at higher data rates. Neither of these effects was included in the analysis reported in Ref. 3. Nevertheless, fair agreement still exists between measurements and predictions.

In addition to rms phase jitter, the steady-state phase error of the Costas loop in the presence of a 2-kHz Doppler offset was also measured for ST/N_0s ranging from −4 to +4 dB. Figure 7 shows the steady-state phase errors of the loops designed for 100 ksps and 250 ksps respectively, with a Doppler offset of 2 kHz. It is observed from Fig. 7 that the measured steady-state phase error of the loop receiving 100 ksps data is in better agreement with theory than that of the loop receiving 250 ksps. This is again due to additional bandlimiting in the complex mixer, which is not accounted for in the analyses, and which introduces additional signal suppression in the loop error signal.

In the actual design of the Costas loop in the Multimegabit Telemetry Demodulator/Detector, the mixer bandwidth will be selected much wider than the data rate to minimize this effect.

IV. Long-Term Stability Tests

To quantify the effects of temperature variations and oscillator long-term instabilities on the reconstructed carrier phase, a long-term stability test in excess of 16 hours has been performed on the Costas loop. The test configuration was the same as that described in Section I. The Costas loop tracks a suppressed carrier BPSK signal with PN data at 100 ksps, and at a ST/N_0 of 4 dB. The loop bandwidth was 110 Hz in this case. The values of the reconstructed carrier phase were recorded and are illustrated in Fig. 8. Each recorded value of the reconstructed carrier phase corresponds to an average of 10,000 samples of the Doppler extractor output, sampling at a rate of 55 ms per sample. Over the 16 hours of observation, the reconstructed carrier phase of the Costas loop was observed to vary not more than 17 deg. This is well within its error budget. In terms of transport delay, a 17-deg phase shift corresponds only to a distance movement of 7 mm at S-Band, and corresponds to an even smaller movement at X-Band.

At another test, the current Block III receiver's residual carrier loop was used to track a residual carrier signal with

modulation angle θ = 80 deg and 100 ksps data on a 360-kHz square-wave subcarrier, at a ST/N_0 of +4 dB. A long-term stability test over a 60-hour period was performed. The reconstructed phase of the residual carrier loop was again recorded and these data are illustrated in Fig. 9. The threshold loop bandwidth setting was 12 Hz in this case. It was observed that the reconstructed phase of the carrier varies over a range 50 deg in this period.

Since these phase variations depend upon the room temperature, no definite conclusion can really be drawn in the above mentioned sample-of-one tests. More tests are planned in the future. Nevertheless it can be said that the phase-shift variation of the Costas loop's reconstructed carrier on a long-term basis is not any worse than that of the current residual carrier loop in Block III, when both loops are operated at the TDL environment.

V. Tracking of Residual Carrier Signals With Data Modulation On a Square Wave Subcarrier

Residual carrier signals are commonly used in the DSN. For example, the Voyager return telemetry uses a modulation angle of 80 deg and data is modulated on a square-wave subcarrier at 360 kHz. To track this type of signal, the arm filters of the Costa loop have to be bandpass filters around the subcarrier frequency to achieve optimum tracking performance. The predicted performance of the Costas loop and the bandpass arm filter design for tracking this type of signal are known.

The test results of the RMS phase jitter of the Costas loop when used to track a residual carrier signal with a modulation angle of θ of 80 deg and a subcarrier at 3.6 times the data rate of 100 ksps are shown in Fig. 10. The arm filters used in this case are RLC bandpass filters centered at the subcarrier frequency. The low-pass equivalents of these filters have a one-pole RC characteristic, and the one-sided bandwidth of this low-pass characteristic is chosen to be at twice the data rate. Also shown in Fig. 10 are the rms jitter measurements of the Costas loop used to track a suppressed carrier signal (θ = 90 deg) with 100 ksps data on the carrier. Comparing these two results, it is observed that the rms phase jitter of the Costas loop tracking of the residual carrier case is about 1-dB worse than those of the suppressed carrier case. This is in fair agreement with the analysis.

Also shown in Fig. 10 is the corresponding rms jitter of the residual carrier loop in the Block III receiver. The loop bandwidth was set to 12 Hz at threshold. The Costas loop tracking is seen to be better than the existing residual carrier tracking over the entire range of ST/N_0 from −4 to +4 dB.

VI. Tests on Asymmetric Bandpass Filtering Effects

In the presence of Doppler offsets, the received signal spectrum will not be centered with respect to the maser amplifier bandpass characteristics. The reconstructed carrier phase of the Costas loop will then depend upon the Doppler offset as well as the maser phase delay characteristics. The same is true for the residual carrier loop. This effect has been analyzed in Ref. 4.

To receive telemetry signals with data rates up to 30 Msps, it is necessary for the X-band maser to have a 1-dB bandwidth around 100 MHz. Since the characteristic of this maser is not yet available we can only make some approximate tests here. In our tests at TDL, a tunable two-pole Tchebycheff bandpass filter with a 0.5-dB ripple in the passband was used to simulate the maser passband characteristic. This filter was placed between the Costas loop and the 10-MHz IF output of the Block III receiver, as shown in Fig. 11. This amounts to an IF simulation of the X-Band maser. The bandpass filter was first designed to be centered at the 10-MHz IF and to have a 1-dB bandwidth of 350 kHz, which is about 3.3 times larger than the received data rate of 100 ksps. After the Costas loop acquired lock, the phase of the reconstructed carrier was recorded from the Doppler extractor output. The filter was then perturbed by adjusting the variable inductor and capacitor elements until the phase of the reconstructed carrier experienced a 37-deg shift. The filter was then recalibrated and the center frequency was determined. Figure 12 plots the amplitude responses of this two-pole Tchebycheff bandpass filter before and after it was perturbed. It was centered at the 10-MHz IF before perturbing. After perturbing, the center frequency was changed to 9.95 MHz. This corresponds to a shift of 50 kHz, which is equal to one half of the 100 ksps data rate that the loop was tracking. According to the analytical result reported in Ref. 4, this frequency shift of the signal carrier with respect to the passband center frequency should have produced a phase shift of 12.5 deg in the Costas loop's reconstructed carrier. However, perturbing the components of the bandpass filter also alter the filter's bandpass characteristic in addition to changing its center frequency. This explains the fact that the measured phase shift is more than the analytical predictions, since the latter assumes no change in the filter bandpass characteristic except for the change in the signal's carrier with respect to the filter's center frequency. Nevertheless, they do indicate a fair agreement. The (future) X-band maser is assumed to have a 1-dB bandwidth of 100 MHz, which is about 3.3 times the

maximum data rate of 30 MHz. In this case, the Doppler offset of half the data rate will amount to 15 MHz. In other words, it will take a Doppler offset of around 15 MHz to introduce a 37-deg shift in the reconstructed carrier of the Costas loop if the maser passband characteristic can indeed be approximated by this two-pole Tchebycheff characteristic. Since realistic Doppler offsets are not greater than 1 MHz, this will imply that the phase shifts in the reconstructed carrier are not a severe problem if we have a wide bandwidth maser.

VII. Conclusions

A Costas loop has been designed, constructed, and installed in the Block III receiver at TDL. Its purpose was to investigate the compatibility of Costas loop demodulation of suppressed carrier BPSK telemetry with the current radio metric system in the DSN. Initial tests with respect to Doppler tracking indicate no noticeable incompatibilities. More tests are planned with respect to ranging compatibility.

References

1. Lesh, J., "Tracking Loop and Modulation Format Considerations for High Rate Telemetry," DSN Progress Report, Vol. 42-44, Jet Propulsion Laboratory, Pasadena, Calif., Jan.-Feb., 1978.

2. Lesh, J., "Functional Requirements Document For Feasibility Model-Multimegabit Telemetry Demodulator/Detector Assembly (MTDD-F)," Memorandum No. 331-79-02, Jet Propulsion Laboratory, Pasadena, Calif., Dec. 29, 1978. (JPL internal document.)

3. Stevens, G., and Woo, K. T., "Design of A Costas Loop to Operate with the Block III Receiver and Its Predicted Performances," this issue of the DSN Progress Report.

4. Woo, K. T., "Effects of Asymmetric Passband Filtering on the Phase of the Costas Loop's Reconstructed Carrier," this issue of the DSN Progress Report.

Table 1. Results of pull-in time tests

Frequency offset, Hz	Predicted values of pull-in time, s	Experimental results of pull-in time, s
100	2.83	3
200	11.3	10
300	25.47	22
400	45.25	39

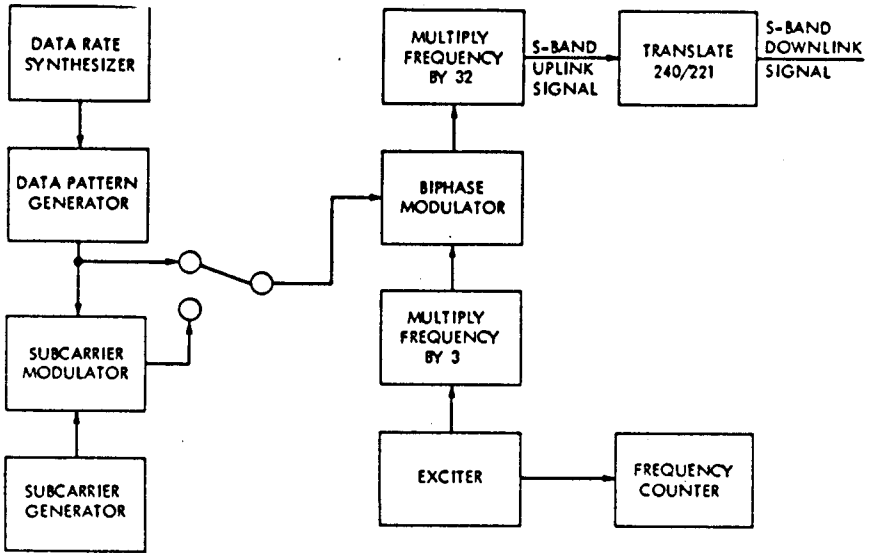

Fig. 1. Transmitter hardware configuration

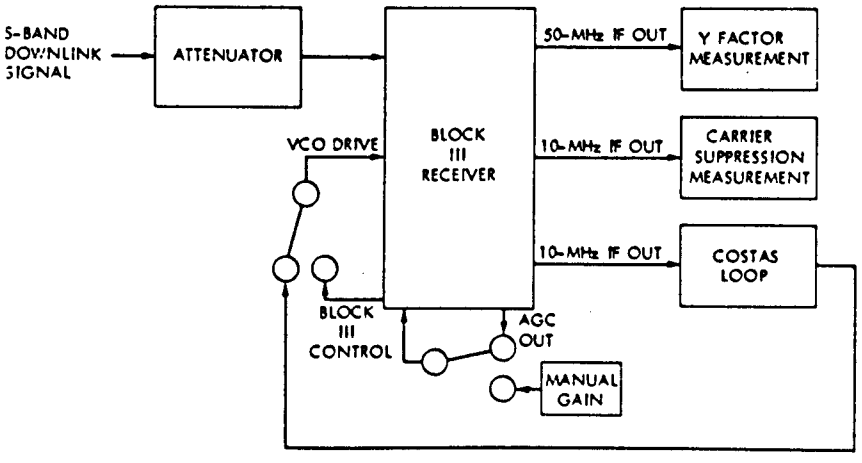

Fig. 2. Receiver hardware configuration

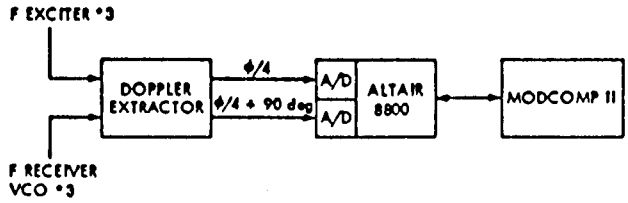

Fig. 3. Data acquisition hardware

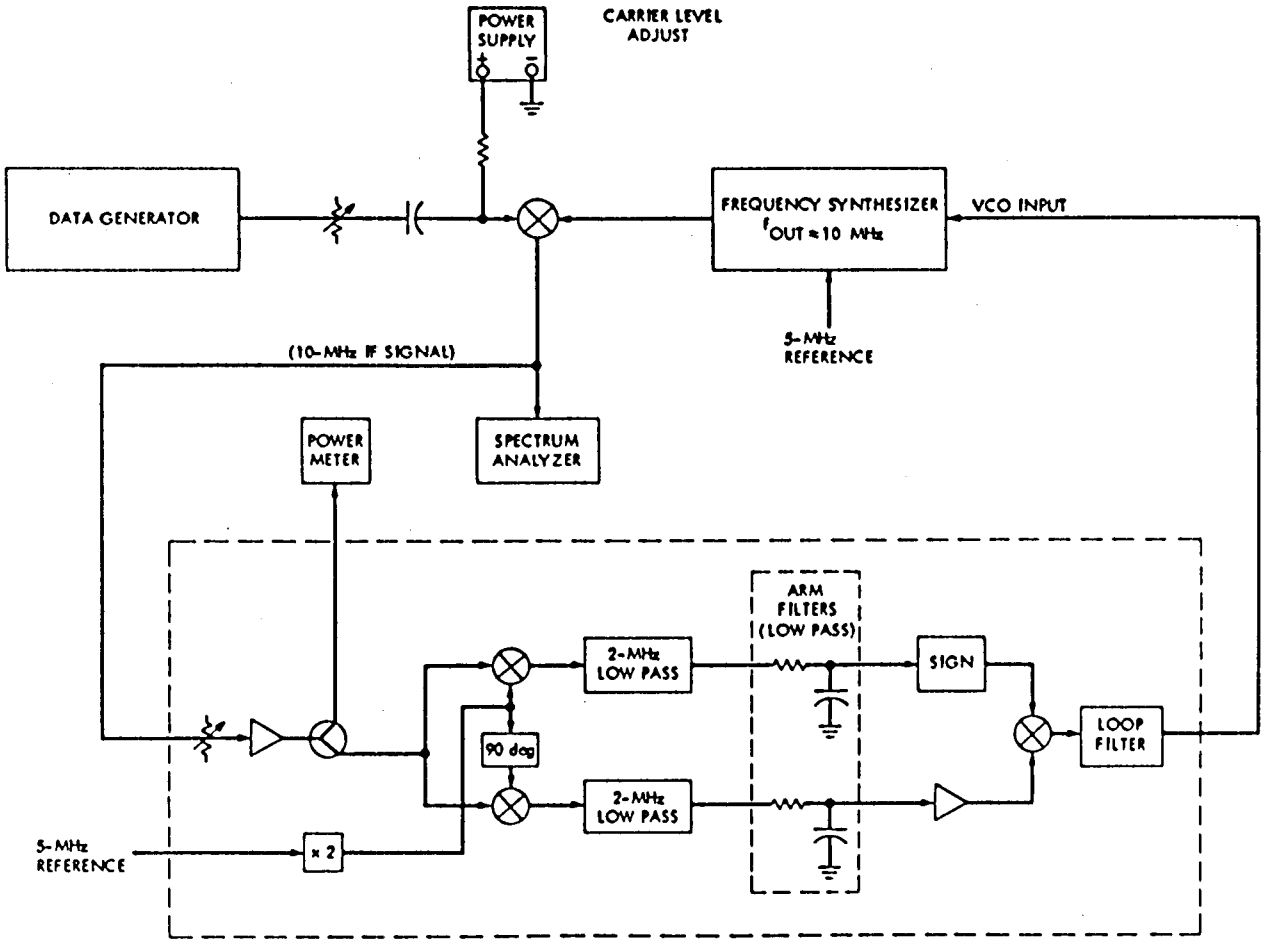

Fig. 4. Costas loop test setup to generate BPSK modulated IF signal

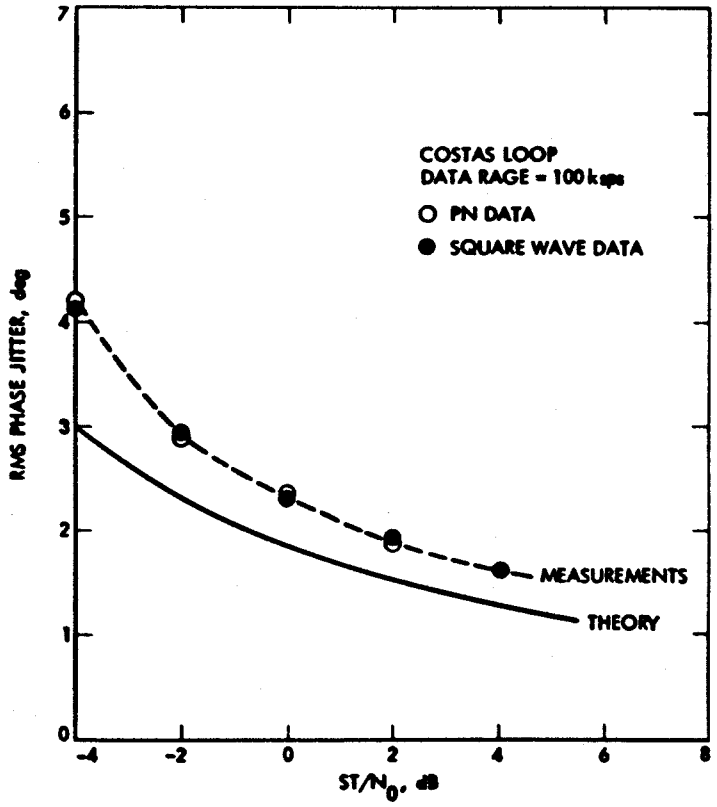

Fig. 5. Rms phase jitter measurements for 100 ksps

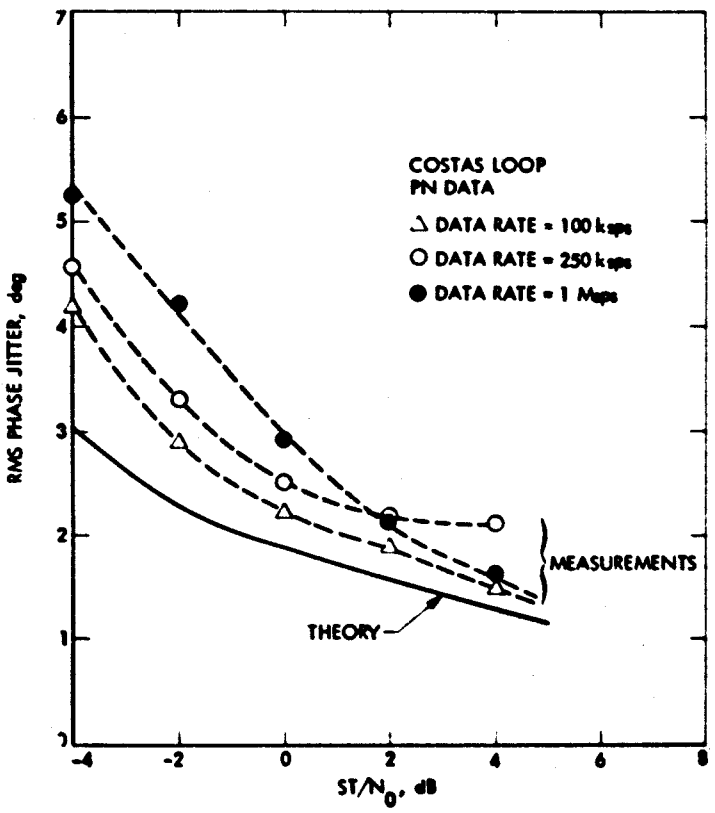

Fig. 6. Rms phase jitter measurements for 100 ksps to 50 ksps, and 1 Msps

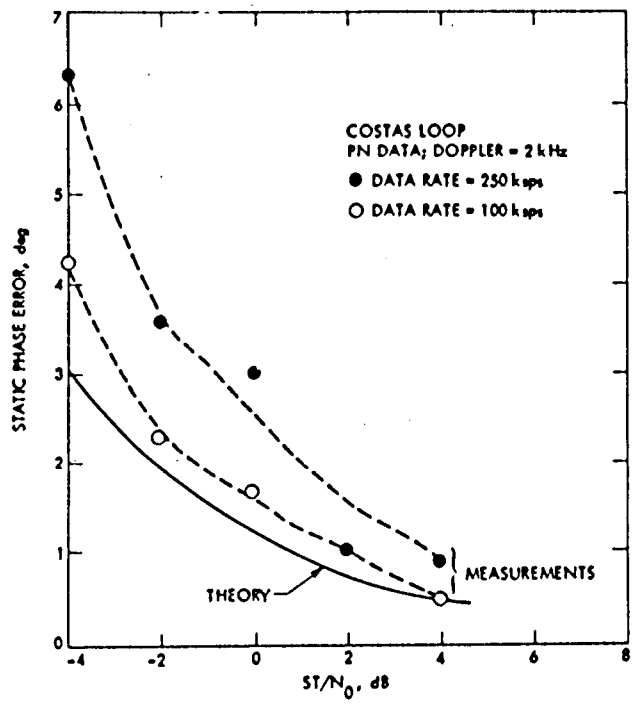

Fig. 7. Steady-state phase error measurements

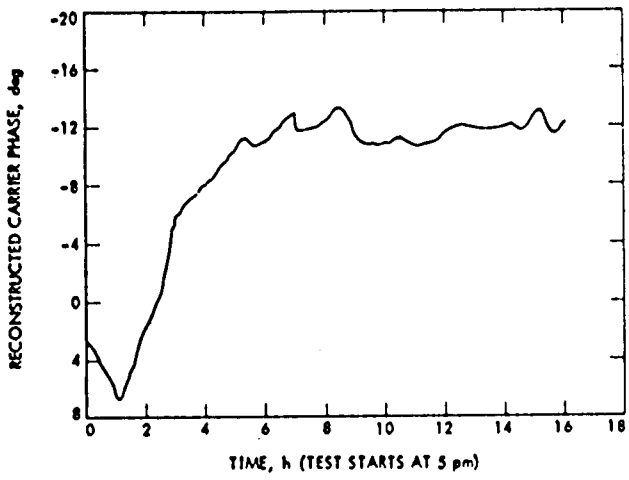

Fig. 8. Long-term stability test results on the Costas loop's reconstructed carrier phase (data rate = 10 ksps, ST/N_0 = 4 dB, suppressed carrier, PN data)

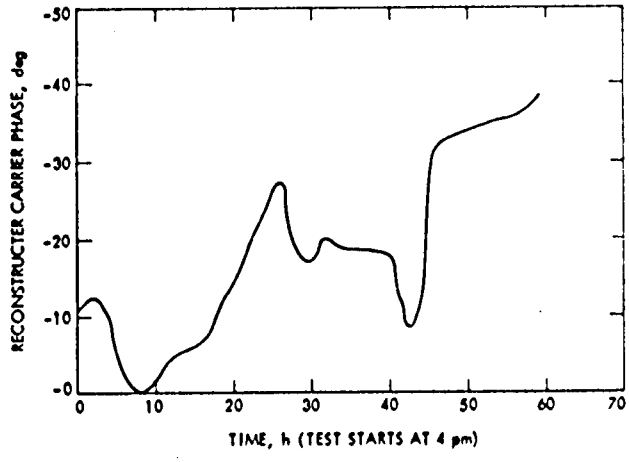

Fig. 9. Long-term stability test results on the Block III residual carrier loop's reconstructed carrier (modulation angle θ = 80 deg, PN data, 100 ksps, data on 360 kHz square wave subcarrier, ST/N_0 = 4 dB

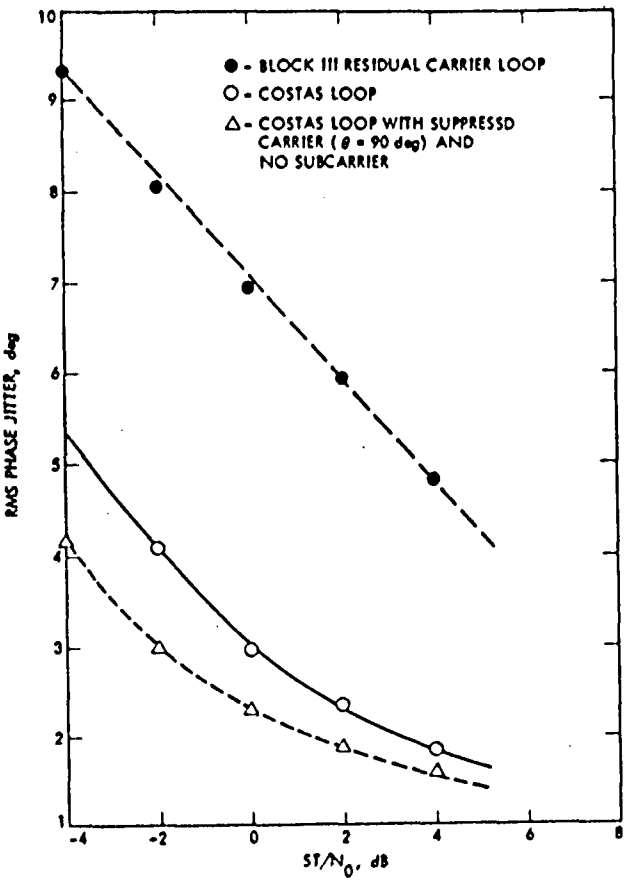

Fig. 10. Residual carrier signalling phase jitter measurements (data rate = 100 ksps, modulation angle θ = 80 deg, subcarrier frequency = 360 kHz)

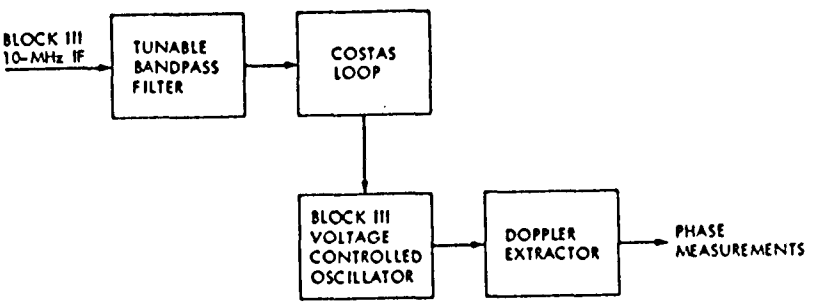

Fig. 11. Test configuration to simulate the effect of receiver front end asymmetric filtering on the phase shifts of the reconstructed carrier in the presence of Doppler shifts

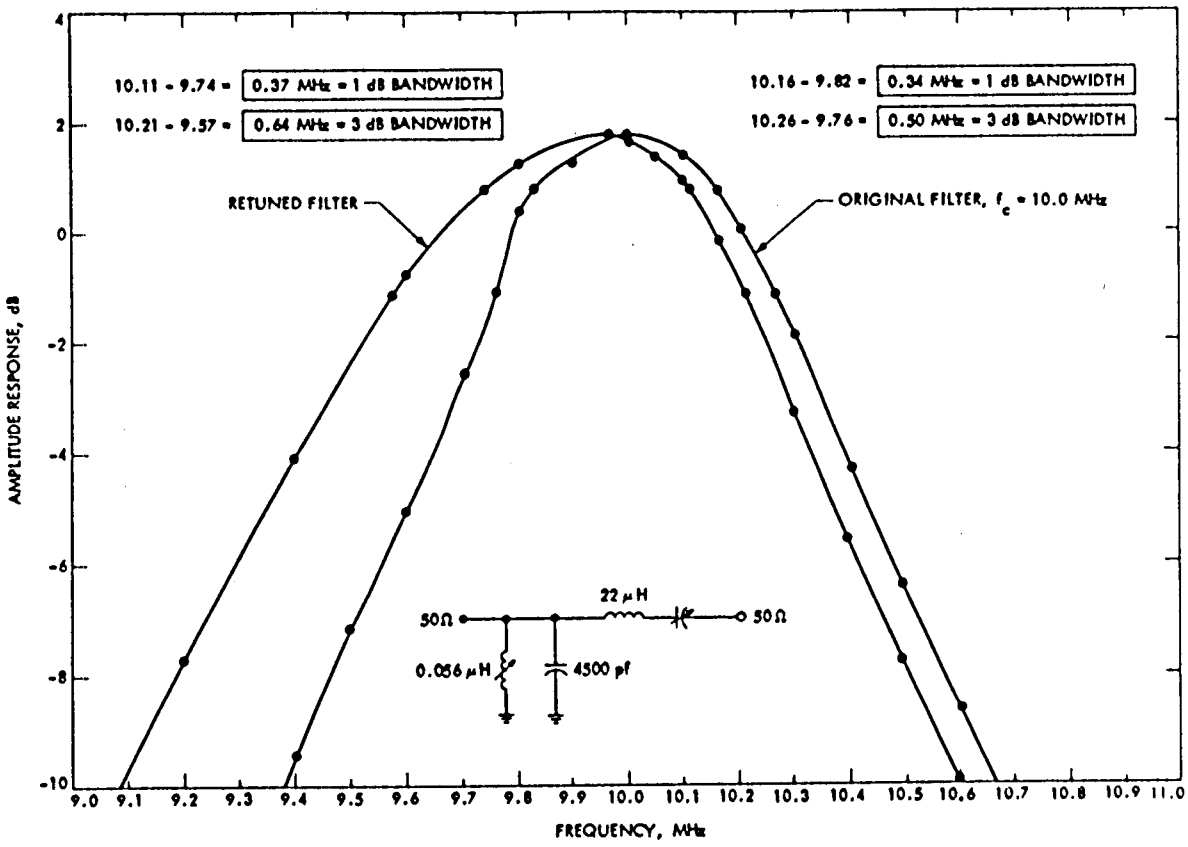

Fig. 12. Amplitude responses of bandpass filter before and after returning